AD-A076 929 TRANSPORTATION SYSTEMS CENTER CAMBRIDGE MA F/G 20/4

CHICAGO MONOSTATIC ACOUSTIC VORTEX SENSING SYSTEM. VOLUME I. DA--ETC(U)

OCT 79 D C BURNHAM

UNCLASSIFIED TSC-FAA-79-18-1 FAA-RD-79-103-1 NL

1 OF 1

AD A076929

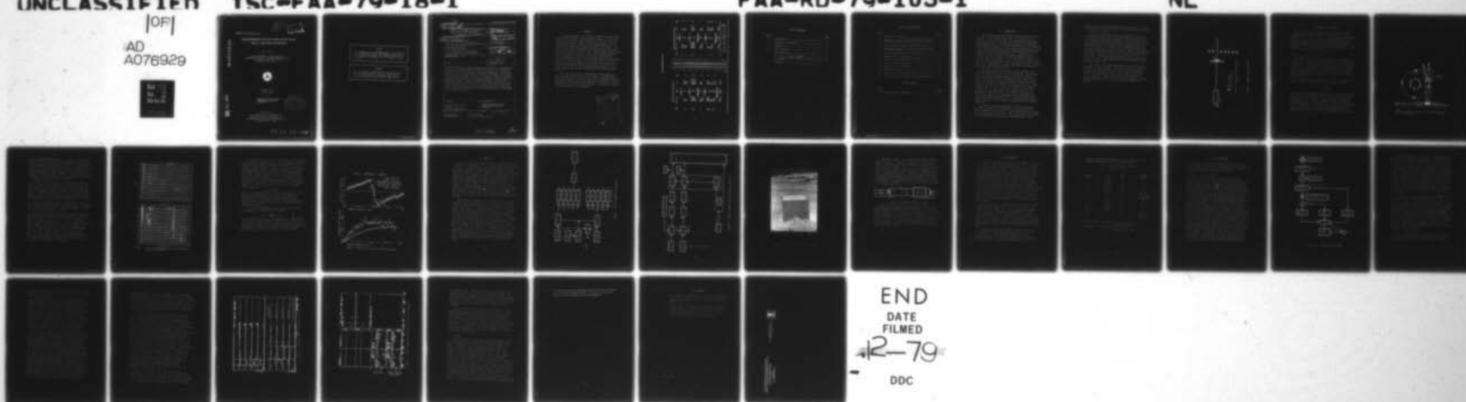

END

DATE FILMED

12-79

DDC

(43) LEVEL II

REPORT NO. FAA-RD-79-103,I

CHICAGO MONOSTATIC ACOUSTIC VORTEX SENSING SYSTEM

Volume I: Data Collection and Reduction

D.C. Burnham

U.S. DEPARTMENT OF TRANSPORTATION
RESEARCH AND SPECIAL PROGRAMS ADMINISTRATION
Transportation Systems Center
Cambridge MA 02142

OCTOBER 1979

FINAL REPORT

Prepared for

U.S. DEPARTMENT OF TRANSPORTATION
FEDERAL AVIATION ADMINISTRATION
Systems Research and Development Service
Washington DC 20591

Technical Report Documentation Page

1. Report No.	2. Government Accession No.	3. Recipient's Catalog No.
18 19 FAA-RD-79-103[redacted]-1		

4. Title and Subtitle	5. Report Date
6 CHICAGO MONOSTATIC ACOUSTIC VORTEX SENSING SYSTEM. Volume I. Data Collection and Reduction.	11 Oct[redacted]79
	6. Performing Organization Code
7. Author(s)	8. Performing Organization Report No.
10 D. C. Burnham	14 DOT-TSC-FAA-79-18[redacted]-1
9. Performing Organization Name and Address	10. Work Unit No. (TRAIS)
U.S. Department of Transportation Research and Special Programs Administration Transportation Systems Center Cambridge MA 02142	FA905/R0132
	11. Contract or Grant No.
	13. Type of Report and Period Covered
12. Sponsoring Agency Name and Address	9 Final Rep[redacted]rt. 16 Jan[redacted]76-Sep[redacted]77
U.S. Department of Transportation Federal Aviation Administration Systems Research and Development Service Washington DC 20591	14. Sponsoring Agency Code

15. Supplementary Notes

12 33

16. Abstract

A Monostatic Acoustic Vortex Sensing System (MAVSS) was installed at Chicago's O'Hare International Airport to measure the strength and decay of aircraft wake vortices from landing aircraft. The MAVSS consists of an array of acoustic antennas which measure the vertical profile up to 60 m altitude of the vertical component of the wind. The decay in wake vortex strength is measured as the vortex passes over successive antennas in the array. Volume I describes the MAVSS principles of operation, the hardware developed, and data reduction methods employed. Volume II (to be published at a later date) analyzes the data collected in order to determine whether B-707 and DC-8 aircraft should continue to be divided into "heavy" and "non-heavy" categories on the basis of wake vortex hazard. Volume III (to be published at a later date) describes the statistical methods used to understand wake vortex decay and presents data on all common jet transport aircraft.

17. Key Words	18. Distribution Statement
Aircraft Wake Vortices Vortices Vortex Strength Decay Acoustic Remote Sensor	DOCUMENT IS AVAILABLE TO THE PUBLIC THROUGH THE NATIONAL TECHNICAL INFORMATION SERVICE, SPRINGFIELD, VIRGINIA 22161

19. Security Classif. (of this report)	20. Security Classif. (of this page)	21. No. of Pages	22. Price
UNCLASSIFIED	UNCLASSIFIED	32	

Form DOT F 1700.7 (8-72) Reproduction of completed page authorized

407082 Jlm

PREFACE

An understanding of the statistical nature of aircraft wake vortex decay can lead to improved airport capacity. The Vortex Advisory System (VAS), about to become operational at O'Hare International Airport, reduces aircraft spacing when the wind conditions are known to eliminate the wake vortex hazard. The VAS is based on data concerning vortex position only and takes no account of vortex strength. This report presents statistically significant data on the decay of wake vortex strength measured with the Monostatic Acoustic Vortex Sensing System (MAVSS). These data could be used to refine the wake vortex aircraft categories (of specific interest is the current division of B-707's and DC-8's into two categories) and to assess the influence of various meteorological conditions on wake vortex decay. The latter analysis may lead to enhancement of the Vortex Advisory System.

The writer would like to acknowledge the contributions of others to the work presented in this Volume. The MAVSS was installed and operated by Illinois Institute of Technology Research Institute (IITRI) who built the MAVSS for one baseline. The data reduction was carried out by John Winkler. Jim Hallock's suggestions on the report are appreciated.

METRIC CONVERSION FACTORS

Approximate Conversions to Metric Measures

Symbol	When You Know	Multiply by	To Find	Symbol
		LENGTH		
in	inches	2.5	centimeters	cm
ft	feet	30	centimeters	cm
yd	yards	0.9	meters	m
mi	miles	1.6	kilometers	km
		AREA		
in^2	square inches	6.5	square centimeters	cm^2
ft^2	square feet	0.09	square meters	m^2
yd^2	square yards	0.8	square meters	m^2
mi^2	square miles	2.6	square kilometers	km^2
	acres	0.4	hectares	ha
		MASS (weight)		
oz	ounces	28	grams	g
lb	pounds	0.45	kilograms	kg
	short tons (2000 lb)	0.9	tonnes	t
		VOLUME		
tsp	teaspoons	5	milliliters	ml
Tbsp	tablespoons	15	milliliters	ml
fl oz	fluid ounces	30	milliliters	ml
c	cups	0.24	liters	l
pt	pints	0.47	liters	l
qt	quarts	0.95	liters	l
gal	gallons	3.8	liters	l
ft^3	cubic feet	0.03	cubic meters	m^3
yd^3	cubic yards	0.76	cubic meters	m^3
		TEMPERATURE (exact)		
°F	Fahrenheit temperature	5/9 (after subtracting 32)	Celsius temperature	°C

Approximate Conversions from Metric Measures

Symbol	When You Know	Multiply by	To Find	Symbol
		LENGTH		
mm	millimeters	0.04	inches	in
cm	centimeters	0.4	inches	in
m	meters	3.3	feet	ft
m	meters	1.1	yards	yd
km	kilometers	0.6	miles	mi
		AREA		
cm^2	square centimeters	0.16	square inches	in^2
m^2	square meters	1.2	square yards	yd^2
km^2	square kilometers	0.4	square miles	mi^2
ha	hectares (10,000 m^2)	2.5	acres	
		MASS (weight)		
g	grams	0.035	ounces	oz
kg	kilograms	2.2	pounds	lb
t	tonnes (1000 kg)	1.1	short tons	
		VOLUME		
ml	milliliters	0.03	fluid ounces	fl oz
l	liters	2.1	pints	pt
l	liters	1.06	quarts	qt
l	liters	0.26	gallons	gal
m^3	cubic meters	35	cubic feet	ft^3
m^3	cubic meters	1.3	cubic yards	yd^3
		TEMPERATURE (exact)		
°C	Celsius temperature	9/5 (then add 32)	Fahrenheit temperature	°F

TABLE OF CONTENTS

LIST OF ILLUSTRATIONS

LIST OF TABLES

1. INTRODUCTION

The Transportation Systems Center (TSC) has had the responsibility for developing vortex sensors which can be used at airports to study aircraft wake vortices generated under normal operating conditions. The Monostatic Acoustic Vortex Sensing System (MAVSS) was the first sensor developed which could measure vortex strength and decay. The MAVSS was initially tested in 1972 at the National Aviation Facilities Experimental Center and subsequently developed at Kennedy Airport.(1) Because of poor hardware reliability, much of the Kennedy MAVSS data were of limited value. In the summer of 1975 the MAVSS was rebuilt at TSC to be much more reliable. It was then used in December 1975 for the B-747 Rosamond Lake tests(2) and then installed at O'Hare Runway 32L. Subsequently, an additional MAVSS was constructed and installed at O'Hare Runway 14R.

Each MAVSS antenna measures the vertical profile of the vertical component of the wind above the antenna. This measurement is particularly appropriate for aircraft wake vortices since the ambient wind has virtually no vertical velocity component. The vertical velocity signature of a vortex is thus easily and accurately measured as the vortex drifts over a MAVSS antenna. The decay of a vortex can be monitored as it passes successively over several antennas located on a baseline perpendicular to the flight path. The primary purpose for the MAVSS data collection at O'Hare Airport was to determine how vortex decay depends on aircraft type and meteorological conditions. Both ends of Runway 32L (i.e., 14R) were instrumented in order to generate data as rapidly as possible under all weather conditions.

The MAVSS baselines were located 610 m from the runway threshold for Runway 32L (see Figure 1), and 472 m from the runway threshold for Runway 14R. The extent of the baseline made use of the available real estate. Only two antennas were located on the starboard side (looking toward the threshold) of the

runway at 61 m and 122 m displacements from the runway centerline. On the port side four (14R) and five (32L) antennas were installed at the same 61 m spacings.

Three additional MAVSS antennas available for the 32L installation were located about 472 m from the runway threshold in an experimental configuration designed to measure vortices which were stalled near the runway centerline. In conjunction with the Ground Wind Vortex Sensing System (GWVSS) anemometer baseline 457 m from threshold (See Figure 1), these MAVSS antennas could allow one to measure the vortex strength by computing the velocity line integral around the vortex. The three MAVSS antennas measure the vertical velocities on the runway centerline and 30.5 m to either side. The GWVSS anemometers measure the horizontal velocities in between. These experimental measurements have not been processed at this time.

The results of the MAVSS data collection at O'Hare will be presented in several volumes. This report, Volume I, documents in detail the sensing system and the data processing methods. Volume II will present the results from a special study of B-707 and DC-8 aircraft which currently fall into two wake vortex weight categories. Volume III will present the results for other aircraft types and will describe the statistical analysis in detail.

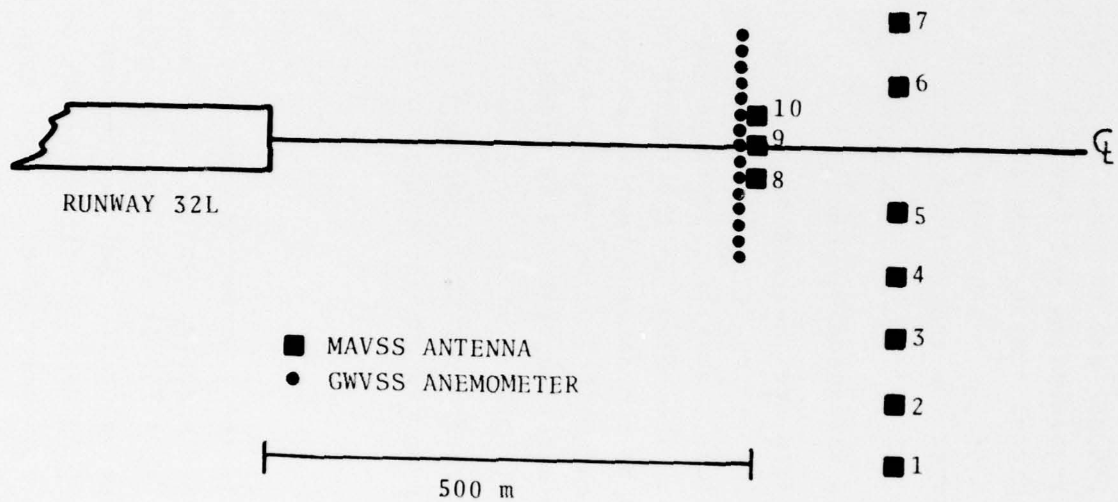

FIGURE 1. RUNWAY 32L INSTALLATION

2. PRINCIPLES OF OPERATION

The MAVSS antenna configuration is illustrated in Figure 2. A short pulse of acoustic energy is transmitted into a narrow vertical beam. Acoustic signals scattered by temperature fluctuations in the air are received by an overlapping receiver beam. Separate transmitting and receiving antennas are employed to prevent antenna ringing from obscuring low altitude returns. The altitude z of the region being probed is determined from the time delay t after the transmitted pulse:

$$z = c\ t/2, \tag{1}$$

where c is the speed of sound.

The data are analyzed by sampling the return signals at various times (i.e., range gates) during the 400-ms period between transmissions. Normally, 16 range gates with 20-ms spacing are processed. The volume of the region contributing to a range gate depends upon the antenna beam width (estimated at 7° full width) and the transmitted pulse width (-6 dB width = 20 ms), the processor integration time (-3 dB width = 16 ms) and the range gate scan time (9 msec).

The average vertical component of the wind in a range gate is measured from the Doppler shifts in the returning signals:

$$v_z = c\ \frac{(\bar{f} - f_o)}{2\ f_o}, \tag{2}$$

where f_o is the transmitted frequency and $\bar{f}$ is the mean frequency of the power spectral density. The mean square deviation of the frequency $\overline{(f - \bar{f})^2}$ is used to give an indication of confidence in the mean value $\bar{f}$. The rms frequency deviation is normally 25 Hz for good data. In the presence of strong velocity gradients (e.g., at the vortex core) or poor signal-to-noise ratios, the frequency deviation becomes larger. The Doppler spectra are analyzed with a real-time spectrum analyzer having a 3 dB width of

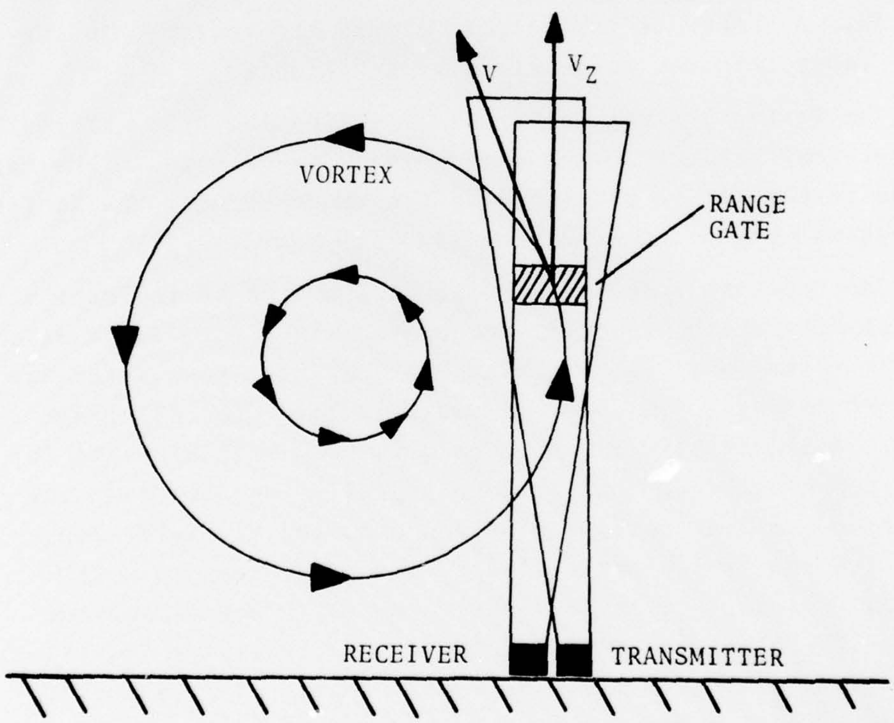

FIGURE 2. MONOSTATIC ACOUSTIC VORTEX SENSING SYSTEM (MAVSS) CONFIGURATION

30 Hz and a sample spacing of 20 Hz. In order to reduce interference between antennas and to simplify data processing, two different transmitted frequencies f_0 are used: 2950 and 3600 Hz. Adjacent antennas have different frequencies. The data from two antennas are mixed together so that three spectrum analyzers operating simultaneously under computer control can process six antennas. A frequency range of ± 280 Hz is scanned, which gives a maximum vertical velocity of 16 m/sec and 13 m/sec respectively for f_0=2950 and 3600 Hz according to Equation 2.

The basic data supplied by a single antenna are shown in Figures 3 and 4. Figure 3 plots the vertical velocity in each range gate versus the time after aircraft passage. Figure 4 plots the mean square frequency deviation $\overline{(f - \bar{f})^2}$ in the same format. The numbers at the left edge of a range gate are half the time (in milliseconds) at which the range gate analysis was started. A number of timing corrections are required to convert this number into the range given by Equation 1.

The vortex arrival in Figure 3 is signaled by a reversal of the vertical velocity components in many range gates. The height of the vortex can be estimated as the range showing the largest velocities before and after the reversal.

The spectral spread data of Figure 4 give an indication of the validity of the velocity measurement in Figure 3. When the ambient noise level is very high, for example, just after the aircraft passage, the spectral width is large for all range gates. A linear time variable gain is used to compensate for the range dependence of the scattered signal. Consequently, the effects of ambient noise are more pronounced at higher ranges. Excessive spectral width will also occur for regions with abnormally small scattered signal, even with normal ambient noise. The other source of excessive spectral width is velocity variations within the MAVSS resolution cell. This effect is generally most pronounced at the vortex core.

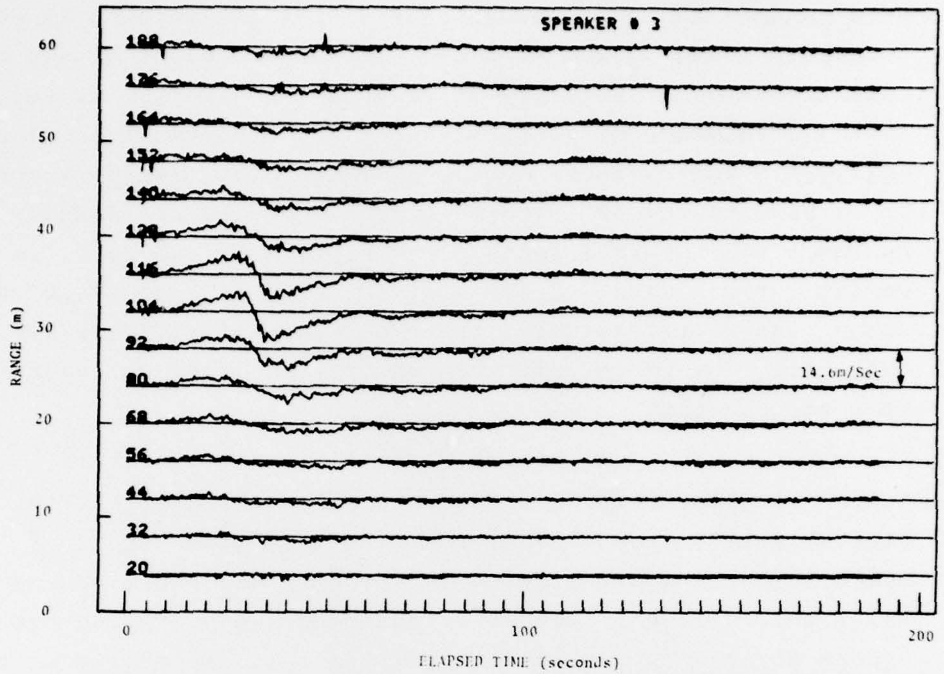

FIGURE 3. VELOCITY VERSUS RANGE GATE AND ELAPSED TIME

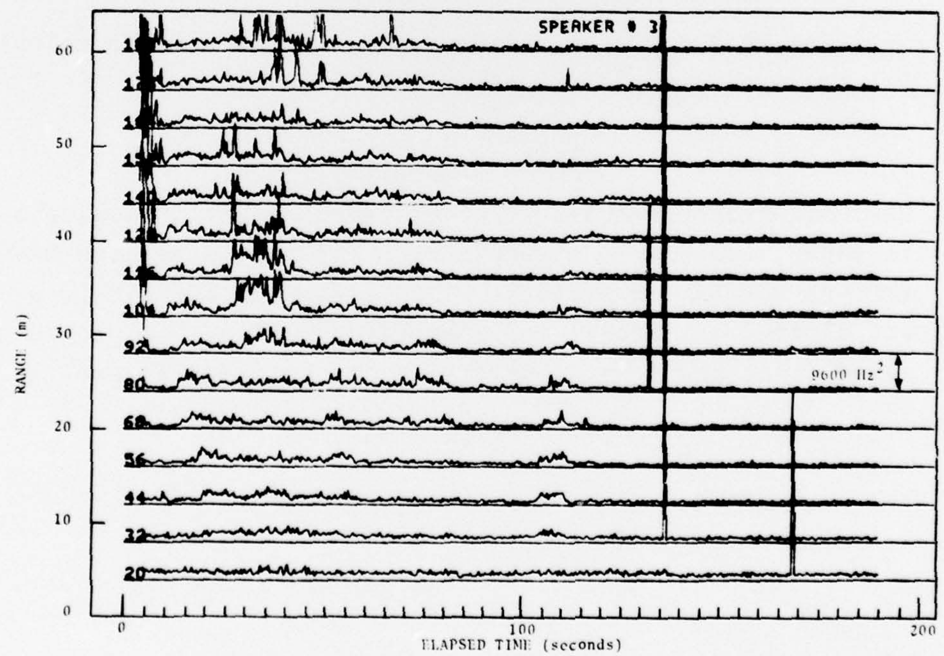

FIGURE 4. MEAN SQUARE FREQUENCY DEVIATION VERSUS RANGE GATE AND ELAPSED TIME

The method of extracting vortex information from the MAVSS data assumes that the vortex passes over the antenna at constant transport speed V_T and at roughly constant height h. In this case the vertical velocity at range z = h directly measures the radial dependence of vortex tangential velocity v(r), assuming negligible vortex decay during passage. The transport speed V_T is used to convert elapsed time since aircraft passage T to radius r via the relationship $r = V_T (T - T_o)$ where T_o is the vortex arrival time. Since a given value of r is observed twice during the vortex passage, the two values of v(r) are averaged together. The vortex circulation $\Gamma_{(r)}$ can then be evaluated from the equation

$$\Gamma_{(r)} = 2\pi r v(r). \qquad (3)$$

Since r is proportional to the estimated value of V_T, the circulation is also proportional to V_T. Thus, this method of measuring vortex circulation is strongly dependent upon V_T being well defined, accurately measured, and large enough to ignore decay. The vortex arrival times at successive antennas are used to estimate V_T.

The method of evaluating vortex strength is to calculate the average vortex circulation up to radius b:

$$\Gamma'(b) = \frac{1}{b}\int_o^b \Gamma_{(r)} dr, \qquad (4)$$

which is proportional to the rolling monument on a wing of span 2b under some simple assumptions. Figure 5 shows the MAVSS data for one vortex; the velocity v(r) and circulation $\Gamma_{(r)}$ profiles are plotted as circles and the average circulation as pulses. The solid lines are least square fits to the velocity profile.

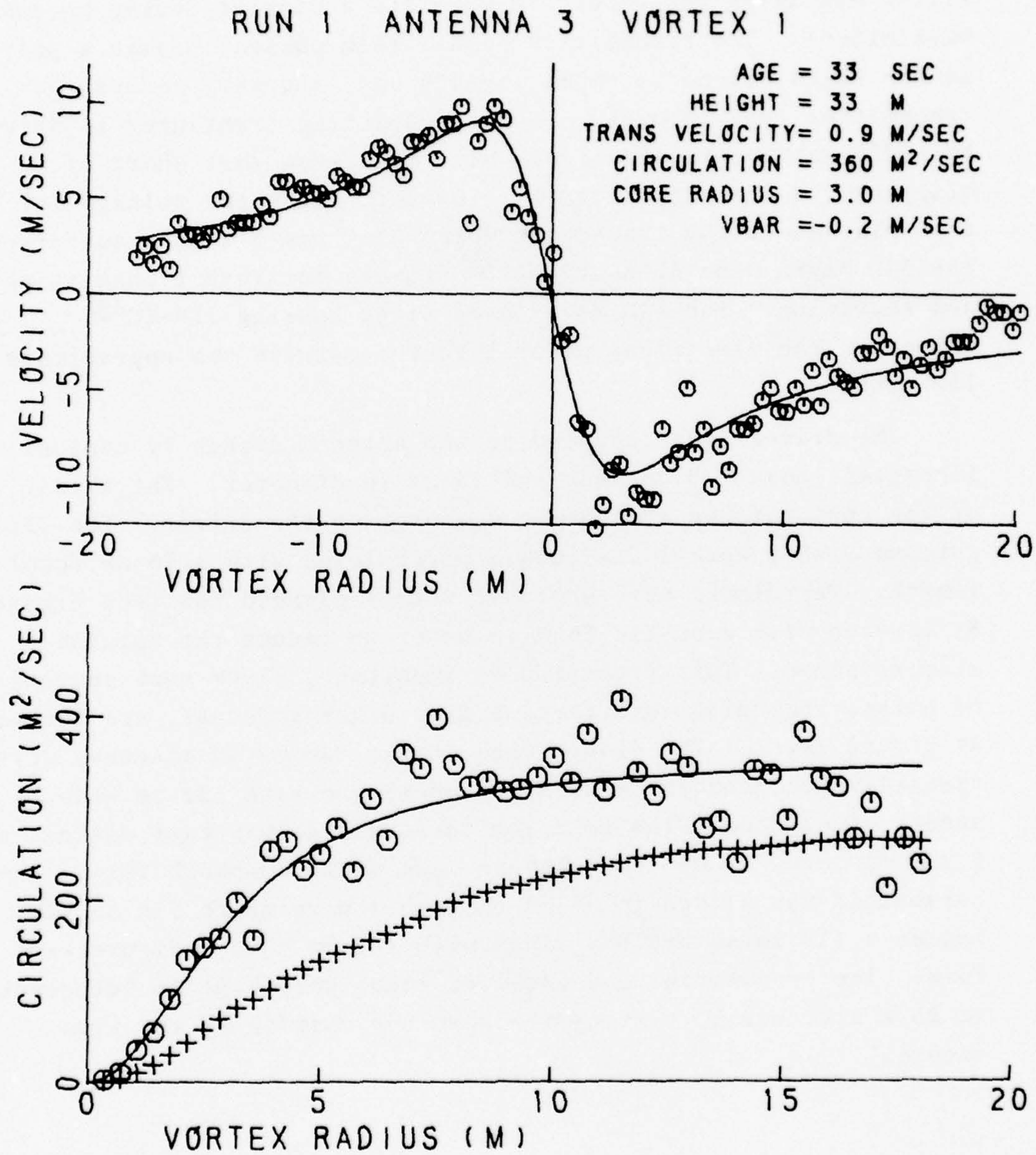

FIGURE 5. VORTEX VELOCITY AND CIRCULATION PROFILES

3. HARDWARE

Figures 6 and 7 show a block diagram of the MAVSS hardware. A crystal clock generates the basic 400 msec period between transmit pulses. A smooth-envelope low-side-band transmitted signal is generated by passing a 20 msec square pulse through a low-pass filter and using the result to modulate a carrier (using an analog multiplier). The transmitted signal then passes through a pair of diodes which attenuate small signals and, thereby, reduce the transmitter feed-through. Each transmitting transducer is driven by a 200 watt power amplifier which is driven just short of clipping. A line transformer is used to raise the voltage for transmission to the transducer which also has a line transformer. The 32L MAVSS used Atlas PD-60T® drivers for both transmitting and receiving. The 14R MAVSS used Altec Lansing 290-4G® drivers. The electrical power into the drivers was approximately 150 watts.

The drivers were coupled to the antenna dishes by conical fiberglass horns 20 cm long and 13 cm in diameter. The throat of the cone matched the output diameter of the driver. The 32L antenna dishes were 1.2 m square paraboloids with a 76 cm focal length. The dishes were enclosed with a plywood box (see Figure 8) covered with acoustic foam in order to reduce the antenna side response. This provision is important, since most sources of noise, including interference from other antennas, are located at ground level. The dishes used in the 14R MAVSS antennas were specially designed for convenient enclosure with 122 cm wide sheets of plywood. The mold for these dishes was cast against a 1.8 m diameter 53 cm focal length spun aluminum paraboloid. The paraboloid was sliced to a 114 cm inch square which fit neatly inside a 122 cm square box lined with 2.5 cm thick polyurethane foam. The transmitter and receiver beams were made to intersect at 25 m altitude by tilting the boxes or displacing the transducers.

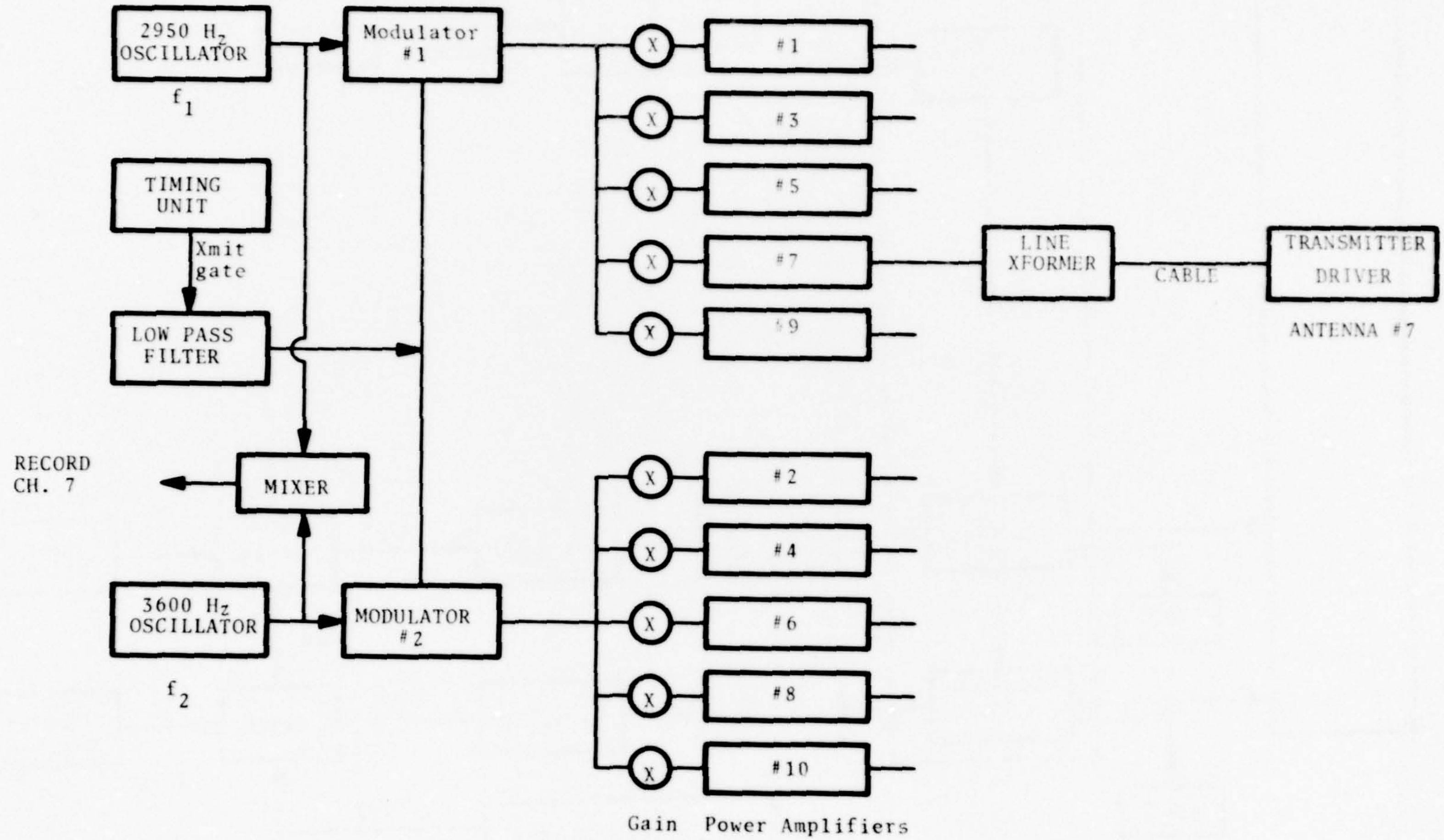

FIGURE 6. MAVSS TRANSMIT ELECTRONICS

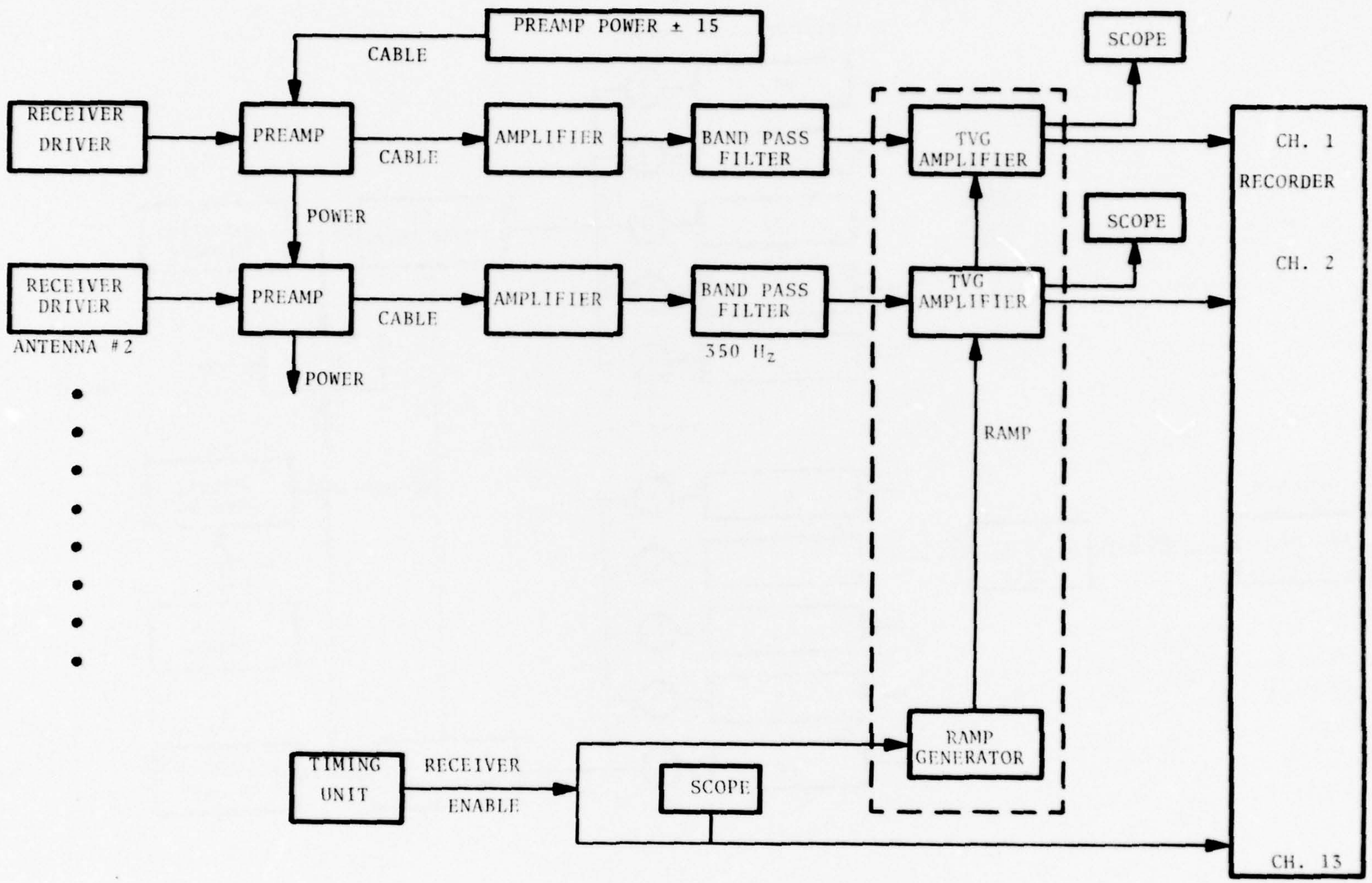

FIGURE 7. MAVSS RECEIVER AND RECORDING ELECTRONICS

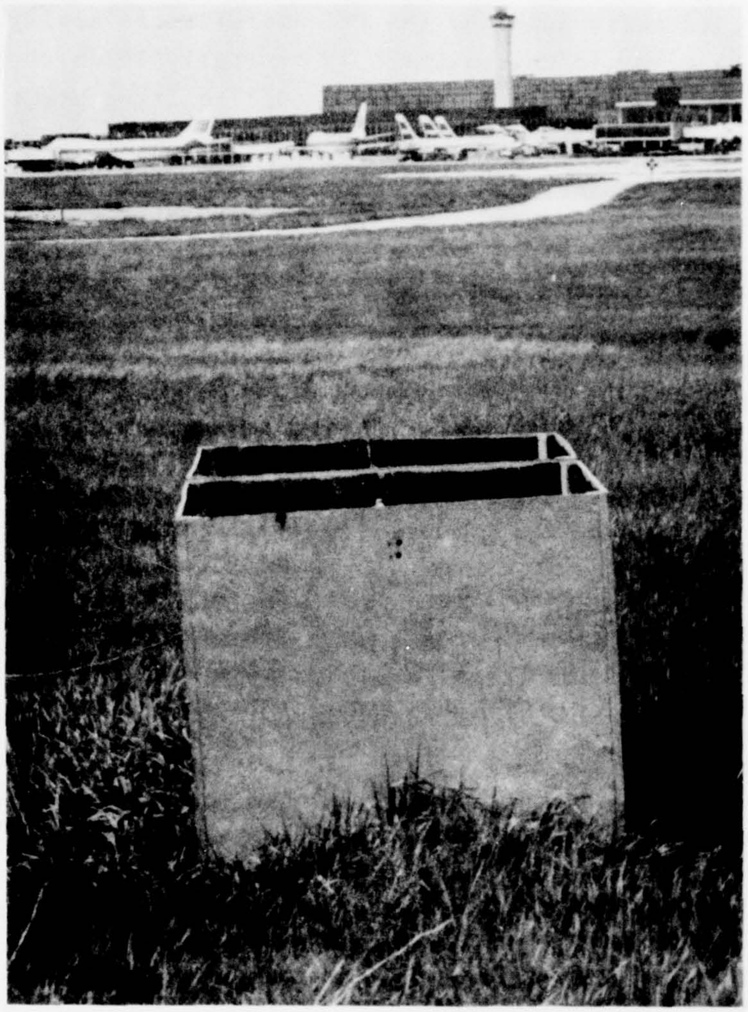

FIGURE 8. ACOUSTIC ANTENNA ENCLOSURES

The receiver signal is first processed by the preamplifier shown in Figure 9. A passive LC tuned (Q=5) high-pass filter serves to attenuate noise below the operating frequency and to raise the signal impedance to 50KΩ. At this impedance level the electronic noise added by the FET amplifier is negligible compared to acoustic noise, which is typically 10 dB above Johnson noise. The high-pass filter is needed to attenuate the strong low-frequency noise component which would otherwise overload the pre-amplifier. The enhanced noise for lower frequencies is due to both greater transducer efficiency and poorer noise shielding by the plywood enclosures.

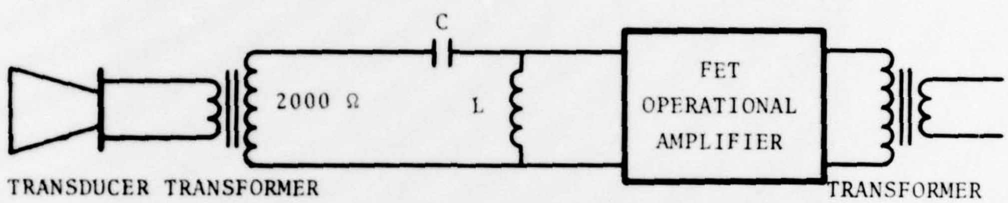

FIGURE 9. PREAMPLIFIER CIRCUIT DIAGRAM

After the pre-amplifier (voltage gain of 100), the signal passes through an impedance reducing transformer and then to the central electronics location via a shielded cable pair. The signal is then amplified with an adjustable gain amplifier and passes through a Q=5 band pass filter (4 pole for the 32L unit, 2 pole for the 14R unit). The signal is then multiplied by a linear ramp in time to correct for the normal range dependence of the backscatter intensity. The signals to be recorded are monitored by a multiscreen oscilloscope.

4. DATA RECORDING

The acoustic data were recorded on a 14 channel instrumentation recorder. The speed of 1-7/8 ips gave 4.4 hours recording for a 2500 foot 10-1/2 inch diameter reel of tape. The channel assignments are shown in Table 1. Four channels were used to record operating information and up to ten channels were available for acoustic data. IRIG B time code was recorded to allow correlation with other data and to enable aircraft runs to be identified by their arrival times. The two transmitted frequencies were recorded CW to allow calibration of the Doppler shifts. A short dc pulse was recorded which was synchronized with the peak in the transmitted signal to give the time reference for the range calculation. A dc pulse was also recorded to indicate when an aircraft passed the antenna array. The duration of this pulse was encoded to give the aircraft type which was input by the operator via a computer terminal. This start-of-run pulse was triggered automatically by detecting the aircraft engine noise.

The acoustic data recording channels were set for 1 percent third harmonic distortion at 1.0 V_{rms} (2.8 V_{pp}) input. The clipping level was about 7 V_{pp}. The system gain was adjusted to give occasional scattered signal peaks above 4 V_{pp} on a sunny afternoon with strong thermal activity. The scattered signal from wake vortices is similar to that obtained under such conditions. The dynamic range for the instrumentation recorder used in the 32L system is 34 dB for 10 kHz band width and, therefore, should be about 46 dB for the 600 Hz band width used in the MAVSS.

The operator turned the recorder on before the arrival of an aircraft and usually recorded continuously as successive aircraft arrived. The recorder was turned off after two minutes when there was a gap in aircraft arrivals. While data were being recorded, the monitor oscilloscopes were set to

display the reproduce outputs from the tape recorder so that proper recording could be verified by the operator.

TABLE 1. RECORDER CHANNEL ASSIGNMENT

Speed = 1-7/8 ips

CHANNEL	TYPE	LEVEL V rms	SIGNAL ANTENNA
1	Direct	1.0	1
2	Direct	1.0	2
3	Direct	1.0	3
4	Direct	1.0	4
5	Direct	1.0	5
6	Direct	1.0	IRIG B Time Code
7	Direct	1.0	Transmitted Frequencies
8	Direct	1.0	6
9	Direct	1.0	7
10	Direct	1.0	8
11	Direct	1.0	9
12	Direct	1.0	10
13	fm	4.0	Sync (2 ms pulse)
14	fm	1.0	Run Start

Direct channels: calibrated level = 1% distortion
3 dB Band width = 10 kHz

FM Channels: calibrated level = 40% deviation
3 dB Band width = 625 Hz

5. DATA PROCESSING

The steps in the data processing are shown in Figure 10. The analog tapes are received at TSC and processed to yield data for entry into a data base. An editing process is included to assure that only valid information is entered.

5.1 PASS 1: SPECTRAL ANALYSIS

The first step in the data processing is the spectral analysis of the data to yield the vertical velocity and the mean square frequency spread. Three real-time spectrum analyzers, Federal Scientific Model UA-15®, are controlled by a Varian 620/L-100 minicomputer system.® The signals from two antennas of different frequency are mixed together and processed by one analyzer. Sixteen evenly spaced range gates are processed in the time between acoustic pulse transmissions (400 ms). In each range gate 28 frequencies around the lower transmitted frequency are processed, followed by 28 frequencies around the higher transmitted frequency. Since the spectrum analyzer requires 0.32 ms for each frequency analyzed, a total of 18 ms are consumed in spectral scanning for each range gate. The analog outputs of the spectrum analyzers are multiplexed, passed through an analog squaring module and digitized by a 9-bit A/D converter. The analog squaring yields the power spectral density directly with no computer overhead. Unfortunately, the dynamic range is reduced to 27 dB, which is much less than the dynamic ranges of recorder (46 dB) and spectrum analyzer (50 dB). In order to regain additional dynamic range, each spectrum analyzer is connected to two multiplexer channels, one of which is preceded by a 16-dB amplifier. The computer then selects the data array having the most suitable gain. The 6x28 word data blocks for each spectral scan are transferred to the computer by direct memory access. The three spectrum analyzers are synchronized in order to allow this efficient way of transferring data.

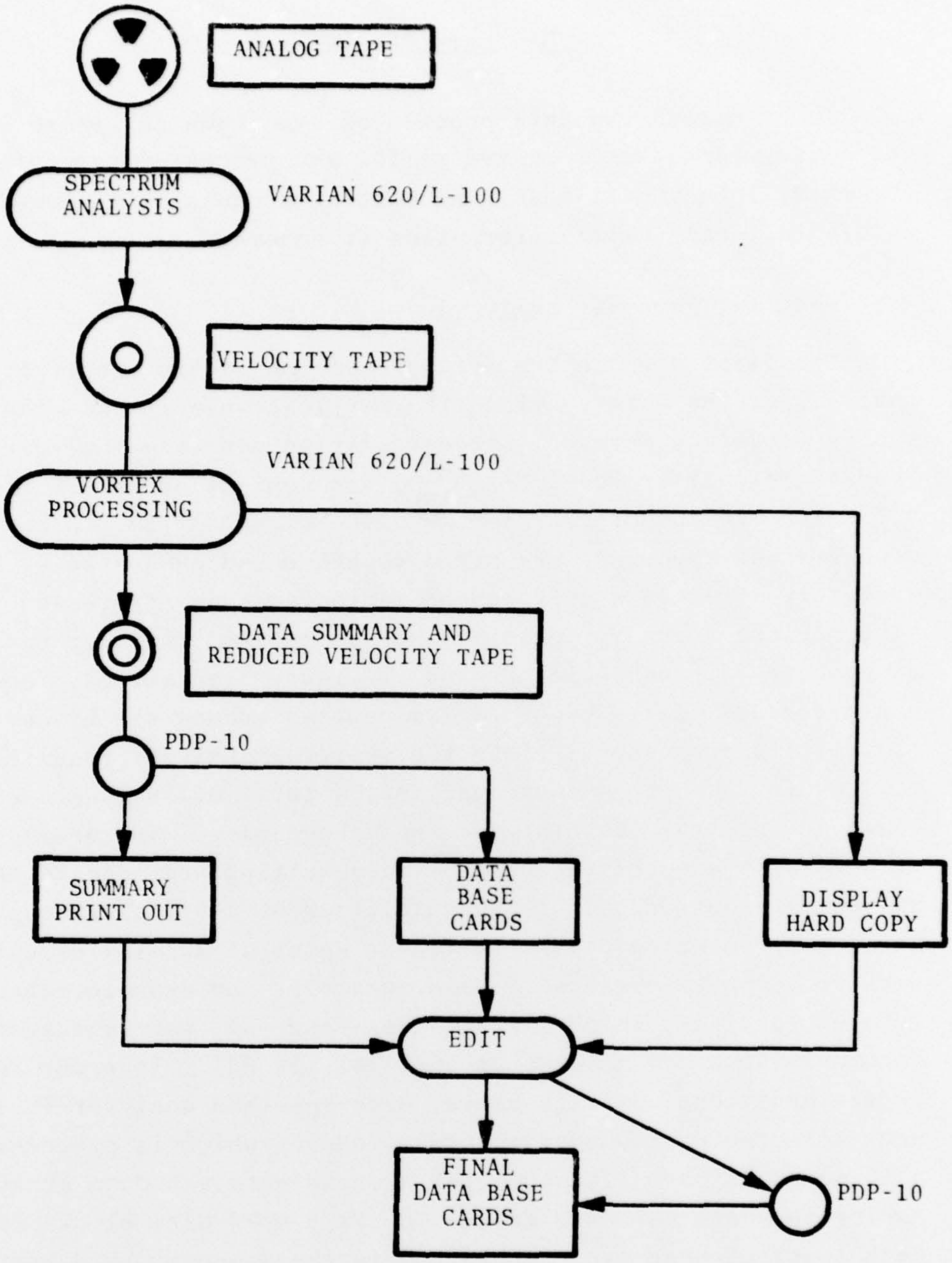

FIGURE 10. MAVSS DATA PROCESSING

The assembly language first-pass processing program calculates the mean frequency of the spectrum and the mean square deviation of the spectrum from the mean. The mean Doppler shift is converted to a velocity which is then output for storage to digital tape 10 inches in diameter. The mean square deviation is also stored as an indication of data quality. The computer also plots the data from a selected antenna on a CRT storage display. The raw frequency spectrum, the velocity, or the mean square frequency deviation can be chosen for display by the operator. The display allows the operator to adjust the gains and mixing levels for the various antennas for the best results. It has not been possible to eliminate the need for a skilled operator at this point in the data processing. The operator also checks the spectrum analyzer calibration, using a program which analyzes and plots the CW transmitted signals recorded on the tape.

The analog tape is reproduced on a Sabre IV® recorder at the real-time speed. The major playback problems have been associated with the two fm channels which process the sync and start-of-run pulse. The positive pulses correspond to increased fm frequency which become more sensitive to the azimuth angle of the playback head. Occasionally, these pulses have dropped out because of incompatible recorder-reproducer head alignment. The amplitude of the pulses was reduced to minimize this effect. (Negative pulses would have been a wiser selection.) The playback system has been plagued with spurious start-of-run pulses from a variety of sources. Therefore, the computer program uses the MAVSS antennas themselves as gating devices in aircraft detection, accepting start-of-run pulses only when much noise is present in the MAVSS spectra.

5.2 PASS 2: VORTEX ANALYSIS

The vortex analysis program processes the velocity and frequency spread digital data tape output of pass 1 to give vortex arrival times and vortex strength. The data output

consists of numerical values and CRT plots showing the vortex detections. The vortex processing program is written in FORTRAN and operates automatically.

The vortex arrivals at an antenna are identified by correlating the velocity data with a function which approximates a vortex signature. It consists of a vertical window 15 m high and a horizontal single-cycle square wave 20 m long. The vertical correlation is obtained by summing the velocities in five range gates. Four overlapping sums are generated for each antenna, as shown in Figure 11. Data points with excessive noise are eliminated from the sums by excluding data with a root mean square frequency spread greater than a set threshold, usually 97 Hz. This threshold is set to reject only very poor velocity data in order to assure that few vortices pass undetected. (The resulting vortex strength may be corrupted by noise and need to be edited out of the final data base.)

The horizontal correlation is more complicated because a specific distance d depends upon the speed with which the vortex passes the antenna. If one assumes constant vortex speed from the runway centerline, the time ΔT for a specific distance to pass the antenna is given by $\Delta T = Td/D$, where T is the vortex arrival time and D is the distance from the antenna to the centerline. The width of the correlator must expand proportionally with the elapsed time. The starting and ending points of this search are set by defining maximum and minimum transport velocities to be considered. The four range sums are searched in this fashion and the most positive and most negative correlations are assigned as the two vortices. In order to avoid spurious signals, the program requires that each sign of the vortex velocity sum contribute at least 20 percent of the correlation and that the correlation must be above a threshold. Another consistency check requires that both vortices have the proper polarity. If the vortex arriving first (designated #1) has the polarity expected for the vortex arriving second (#2), then the vortex having the smaller magnitude correlation is

rejected and another search is conducted over the appropriate times with respect to the vortex retained. The vortex arrival times are indicated in Figure 11 by a vertical line with a slash through the range sum where the extreme value occurred. The vortex height is further refined by searching for the range gate giving the largest correlation with a single-cycle square wave. The velocity and frequency spread profiles for this range gate are plotted in Figure 12.

The vortex transport velocities needed to transform time into vortex radius are obtained by making use of the vortex arrival times at successive antennas. The average transit velocity between two antennas is simply the antenna separation divided by the difference in arrival times. The vortex detections are ordered by the distance of the antennas from the runway centerline. If only one vortex detection is obtained, the transport velocity is estimated assuming the vortex was generated at the centerline and moved out at constant velocity. Such vortices have low accuracy and are designated in the data base with a (1) standing for a one-antenna transport velocity. If more than one detection is made for a particular vortex, the transport velocity for the first and last antennas is given by the average transit time to the adjacent antenna. These vortices have intermediate reliability and are designated with a (2) indicating two-antenna transport velocity. If an antenna has two adjacent detections, the transit velocities to each are averaged to give the most reliable transport velocity. The vortices are marked with a (3) indicating a three-antenna transport velocity. The calculated transit velocities between antennas are used only if they fall within a physically reasonable range. The transport velocities are calculated to a resolution of 0.1 m/sec.

Figure 12 also contains plots of the vortex height and lateral position as a function of time. The final step in the vortex data processing is the calculation of average circulation Γ' for four radii, 5, 10, 20, and 30 m. The values for positive and negative radii must both be present and they are averaged

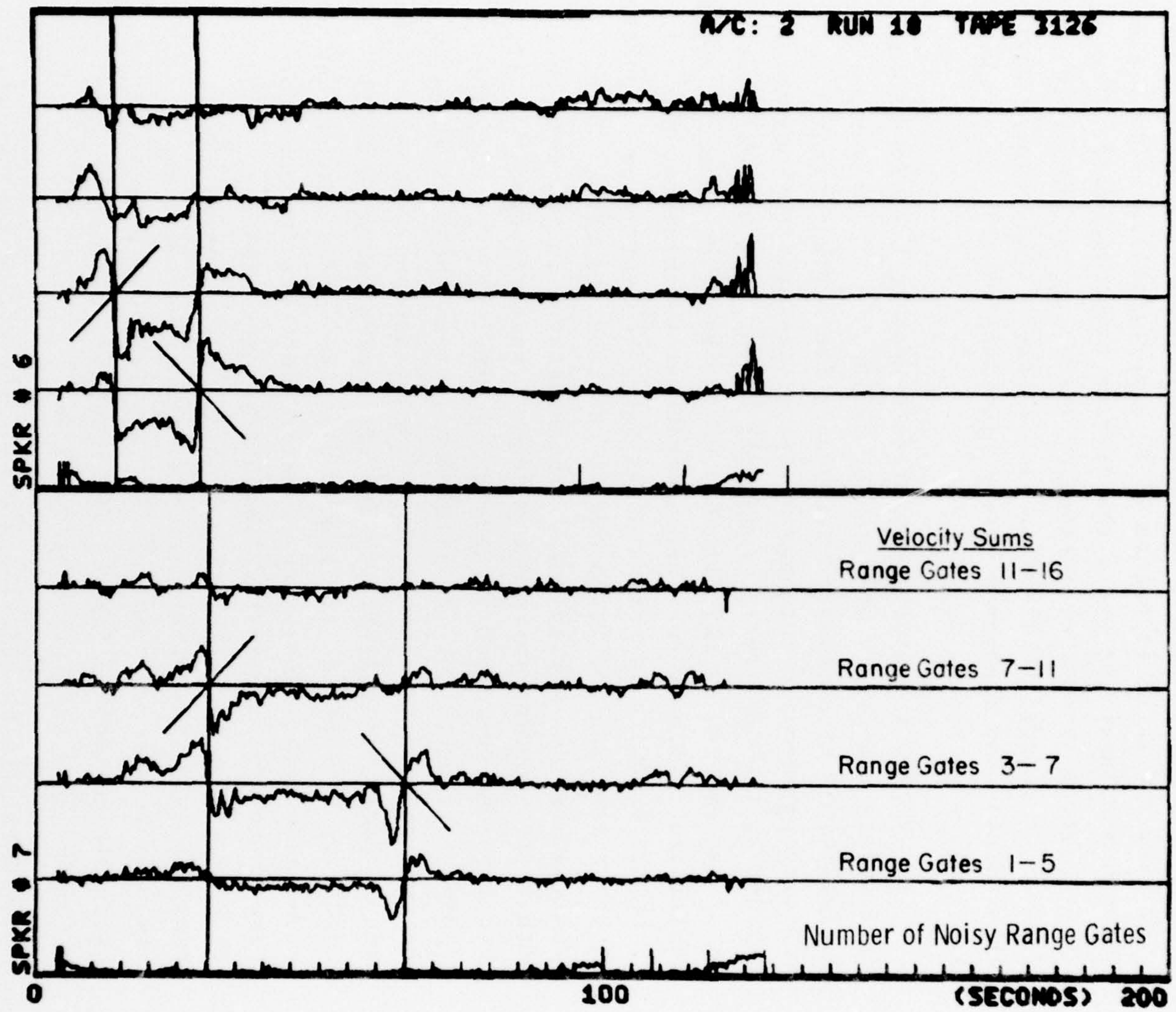

FIGURE 11. DATA FOR VORTEX SEARCH ALGORITHM

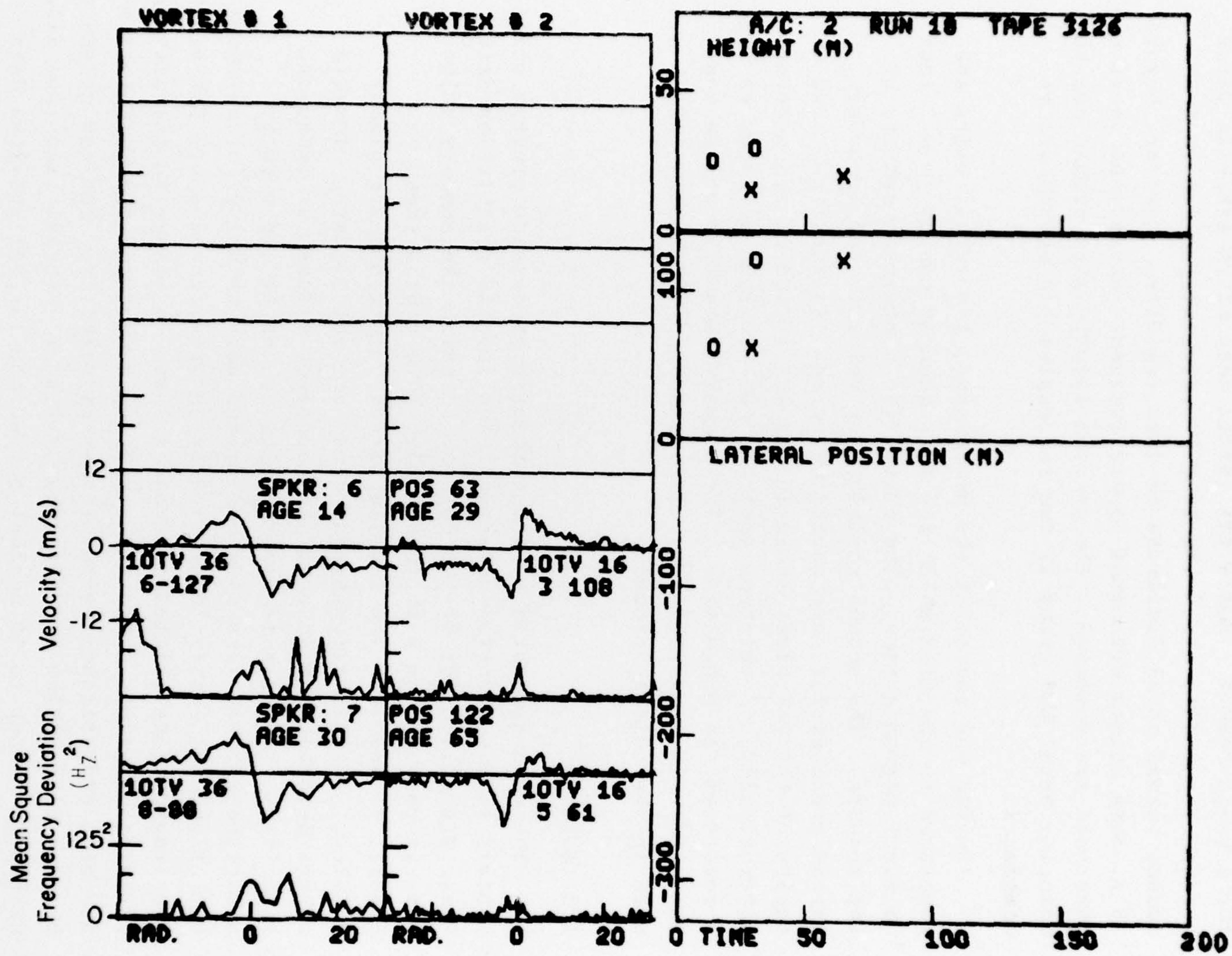

FIGURE 12. VORTEX PROFILES AND TRACKS FOR DETECTED VORTICES

for a valid result. Since the vortex core often exhibits large frequency spreads, the 5 and 10 m Γ' calculations ignore frequency spread as an indicator of data validity. However, beyond 10 m, data points with mean square frequency deviations above the threshold are rejected. The program interpolates around one bad velocity point but stops if two successive bad points are encountered.

During the course of the processing, two output files are generated on the disk which are subsequently copied to a 7-inch diameter magnetic tape. The first file contains a summary of the results. The second contains the velocity and frequency spread profiles for each vortex detected. In addition, hard copies of the CRT plots shown in Figures 10 and 11 are generated automatically. A teletype records "bookkeeping" messages to keep a record of the processing. The summary data file on the magnetic tape is converted to a listing and punched cards, which are used in the editing process.

5.3 EDITING

The data generated by the automatic processing program still contain spurious vortex detections and invalid circulation data. These are edited out of the data by scanning the summary printouts in conjunction with the display hard copies shown in Figures 11 and 12. The invalid vortex detections are simply deleted. Invalid circulation values are set to zero. Invalid vortex detections also generate incorrect values for transport velocities. Often a transport velocity can be improved by using the arrival time of a vortex too weak or noisy for automatic detection, but easily identified by an experienced eye. Correcting the transport velocities also necessitates a change in the average circulation values since the averaging radius and the circulation are both proportional to the transport velocity. The new values of average circulation are obtained by linear interpolation (and also extrapolation up to 10 percent beyond the largest previous data point). If the average circulation is proportional to the averaging radius, as is often the case for small radii, this correction leaves

the average circulation unchanged since the effects of transport velocity on both parameters cancel. The final corrected set of data cards is incorporated into the data base.

6. REFERENCES

1. D.C. Burnhan, T.E. Sullivan, and L.S. Wilk, "Measurement of Wake Vortex Strength by Means of Acoustic Back Scattering," Journal of Aircraft, Vol. 13, No. 11, Nov 1976, p. 889-894.

2. D.C. Burnham, J.N. Hallock, I.H. Tombach, M.R. Brashears, and M.R. Barber, "Ground-Based Measurements of the Wake Vortex Characteristics of a B-747 Aircraft in Various Configurations," Report No. FAA-RD-78-146, Dec 1978, DOT Transportation Systems Center, Cambridge MA.

220 copies

U.S. DEPARTMENT OF TRANSPORTATION
RESEARCH AND SPECIAL PROGRAMS ADMINISTRATION
TRANSPORTATION SYSTEMS CENTER
KENDALL SQUARE, CAMBRIDGE, MA. 02142

OFFICIAL BUSINESS
PENALTY FOR PRIVATE USE, $300

POSTAGE AND FEES PAID
U.S. DEPARTMENT OF TRANSPORTATION
613

U.S. MAIL